

Combinatorial Efficacy Achieved Through Two-Point Blockade within a Signaling Pathway—A Chemical Genetic Approach

Qi-Wen Fan,^{1,2,3,4} Kimberly Musa Specht,^{4,5} Chao Zhang,^{4,5} Dmitriy D. Goldenberg,^{1,2,3,4} Kevan M. Shokat,^{4,5} and William A. Weiss^{1,2,3,4}

Departments of ¹Neurology, ²Pediatrics, ³Neurological Surgery and Brain Tumor Research Center, ⁴Cancer Center, and ⁵Cellular & Molecular Pharmacology, University of California, San Francisco, California

ABSTRACT

Whether the apparent efficacy of a specific kinase inhibitor is attributable solely to inhibition of its primary target, or to combined inhibition of additional unidentified kinases, is a critical issue in cancer therapy. We used a chemical genetic approach to generate a selective inhibitor of *v-erbB* [a transforming allele of *epidermal growth factor receptor (EGFR)*] and interrogated inhibition in known downstream signaling pathways. On the basis of this analysis, we hypothesized that dual inhibition of *v-erbB* and phosphatidylinositol 3' (PI3) kinases could show improved potency. We, therefore, used two different cell lines to examine the effects of *v-erbB* or EGFR inhibitors, in combination with PI3 kinase inhibitors, in mouse models for EGFR-driven cancers. When treated with NaPPI, *v-erbB-as1*-transformed fibroblasts showed cell-cycle arrest and decreased activity of Akt kinase. Inhibitors of *v-erbB-as1* and of PI3 kinase showed enhanced efficacy in treating established 3T3:*v-erbB-as1* tumor allografts. We extended these results to the human glioma cell line U87:MG transduced with Δ EGFR, a tumor-derived activated allele, treating tumor-bearing mice with vehicle, the EGFR inhibitor ZD1839, LY294002, or ZD1839 plus LY294002. In human glioma xenografts, inhibition of EGFR cooperated similarly with inhibition of PI3 kinase. Our experiments provide a preclinical mechanistic basis for combining biologically based therapies directed against two targets within a complex signaling cascade.

INTRODUCTION

Small molecule inhibitors of signaling pathways activated in cancer hold great promise for therapy (1). The introduction of targeted therapeutics into cancer therapy brings with it questions relating to the optimal use of such agents, which therapies should be used for which specific cancers, and how many redundant pathways exist in signaling pathways, and which combinations of drugs will show combinatorial efficacy. Unlike genetic analysis of signaling pathways in cancer, where gene knockouts are able to precisely remove a single protein in a whole animal, small molecule inhibitors are typically not perfectly specific for a single target (2). Moreover, in the area of protein kinase inhibitors, the conserved nature of the ATP-binding pocket essentially precludes developing such agents. Fortunately, anecdotal evidence has suggested that this lack of specificity may lead to enhanced efficacy in situations where a single agent targets multiple cancer-related pathways (3). Conversely, however, nonspecific inhibition may cause dose-limiting toxicities, thereby compromising the utility of some targeted therapies in the treatment of cancer.

The protein kinases represent an extremely large protein family (>800 human protein kinases) of closely related ATP-binding sites that are attractive targets for cancer therapy (4). However, a major

problem with the development of kinase-directed therapeutics is that the vast majority of all protein kinase inhibitors are capable of inhibiting multiple cellular protein kinases (2). For example, separate reports recently tested the ability of two different irreversible inhibitors of epidermal growth factor receptor (EGFR) to block tumor formation in *Apc^{min}* mutant mice. Although both of these inhibitors blocked phosphorylation of EGFR (5, 6), only one of the two inhibitors prevented the development of intestinal neoplasia in this model (5). In a related study, *Apc^{min}* mice mutant at *egfr* also showed decreased development of tumors (7). One interpretation of these disparate reports is that the effective inhibitor was impacting the activity of other unidentified kinases in addition to EGFR. Because the ATP-binding sites are so conserved, small changes to a putative inhibitor of EGFR are likely to affect interactions with other targets and impact these issues. Subtle changes to the structure of kinase inhibitors may affect their potency on a variety of kinases present in the body. For most such kinases, no assay exists through which to test the response to a given inhibitor.

Complicating this situation is the fact that the pathways in which kinases function are highly adaptable and show exquisite compensation when pathways are analyzed by gene knockouts or dominant negative perturbations. To assess the effect of a true drug-like molecule on specific inhibition of a single oncogenic kinase, we turned to a chemical genetic approach. Analogue sensitive engineered kinases can be selectively blocked using inhibitors that are specific to the manipulated kinase. Animal models generated from such analogue-sensitive kinases can be used to assess the impact of selective inhibition and to determine specific from nonspecific effects of small molecule inhibitors.

Although small molecule inhibitors of lipid kinase and the Ras-Raf kinase pathways have been described and characterized, the testing of such agents in combination, and the elucidation of underlying mechanisms through which particular combinations may show improved efficacy are critical to guide the optimal use of such small-molecule inhibitors. Furthermore, through the use of *v-erbB-as1*/NaPPI model system which allows for monospecific inhibition of a single kinase, the true mode of action is known, providing invaluable information about the effect of specific modulators of specific targets in cancer therapy.

Treatment studies in animal systems may be relevant to human cancers by identifying critical targets impacted either by mono- or poly-specific inhibitors and by determining the impact of poly-specific inhibition using combinations of mono-specific targeted therapeutics.

The epidermal growth factor receptor is commonly amplified in glial tumors and is over-expressed in a broad range of malignancies. Identification of *v-erbB* as an activated allele of *EGFR* has provided one of the first links between an activated oncogene and the development of cancer (8). To truly map the cellular effects of inhibiting a specific kinase in a disease context, we used protein engineering to sensitize *v-erbB* to be specifically inhibited by the pyrazolopyrimidine-based ATP competitive inhibitor 1-Naphthyl-PP1. We substituted alanine in place of a conserved threonine within the ATP-binding

Received 7/21/03; revised 10/9/03; accepted 10/15/03.

Grant support: This work was supported by Grants U01CA84290, 1P50CA097257-01, NIH-CA-70331, and NIH-AI-44009 and by grants from Accelerate Brain Cancer Cure and the Brain Tumor Society.

The costs of publication of this article were defrayed in part by the payment of page charges. This article must therefore be hereby marked *advertisement* in accordance with 18 U.S.C. Section 1734 solely to indicate this fact.

Supplementary data for this article are available at *Cancer Research Online* (<http://cancerres.aacrjournals.org>).

Requests for reprints: William A. Weiss, Department of Neurology, University of California, 521 Parnassus Avenue, San Francisco, CA 94143-0663. E-mail: weiss@cgl.ucsf.edu.

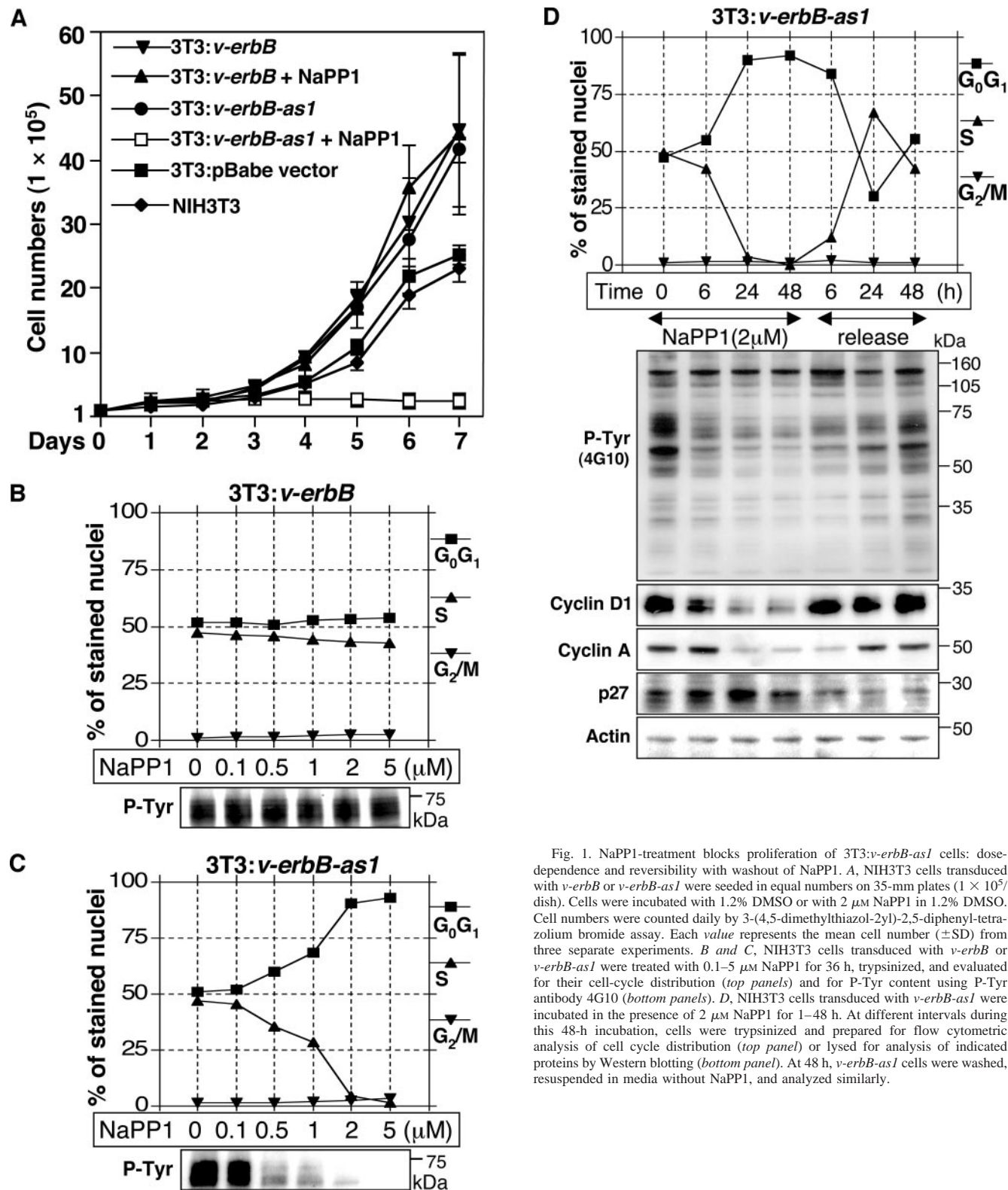
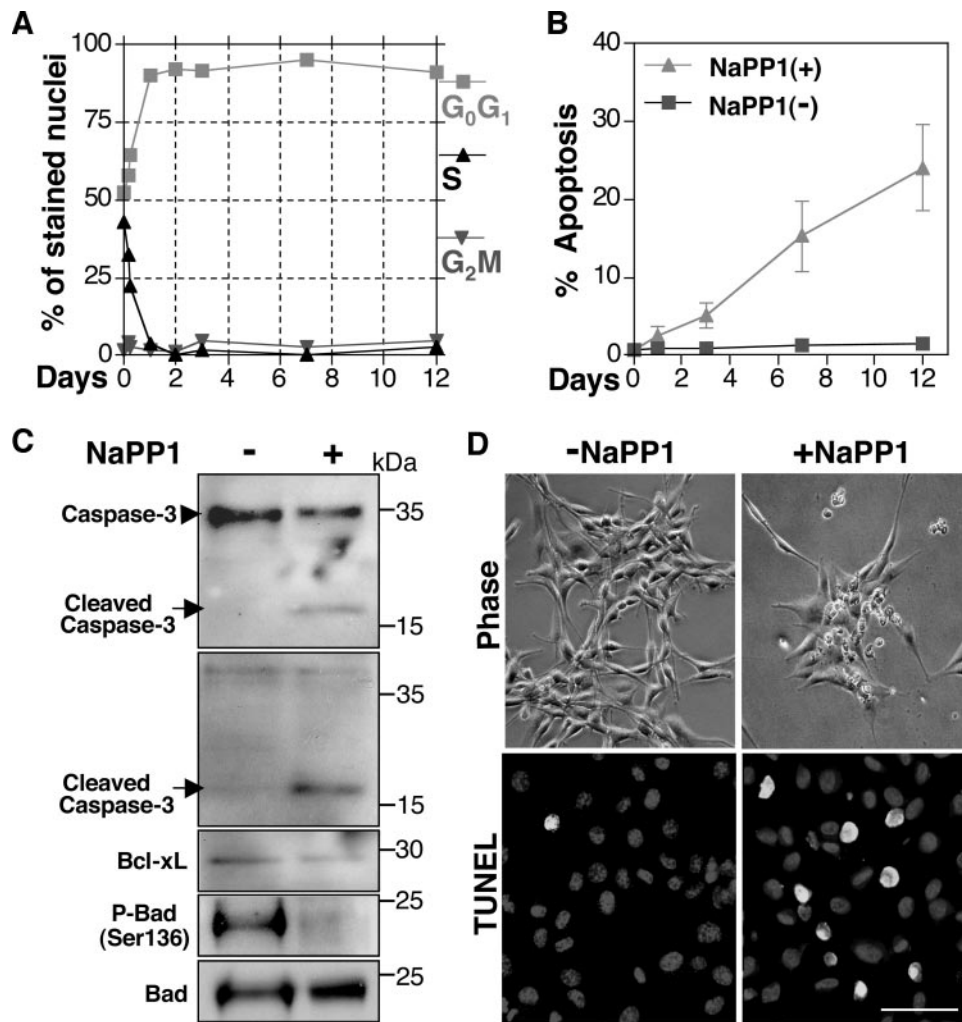


Fig. 1. NaPP1-treatment blocks proliferation of 3T3:*v-erbB-as1* cells: dose-dependence and reversibility with washout of NaPP1. **A**, NIH3T3 cells transduced with *v-erbB* or *v-erbB-as1* were seeded in equal numbers on 35-mm plates (1×10^5 /dish). Cells were incubated with 1.2% DMSO or with $2 \mu\text{M}$ NaPP1 in 1.2% DMSO. Cell numbers were counted daily by 3-(4,5-dimethylthiazol-2-yl)-2,5-diphenyl-tetrazolium bromide assay. Each value represents the mean cell number (\pm SD) from three separate experiments. **B** and **C**, NIH3T3 cells transduced with *v-erbB* or *v-erbB-as1* were treated with 0.1– $5 \mu\text{M}$ NaPP1 for 36 h, trypsinized, and evaluated for their cell-cycle distribution (top panels) and for P-Tyr content using P-Tyr antibody 4G10 (bottom panels). **D**, NIH3T3 cells transduced with *v-erbB-as1* were incubated in the presence of $2 \mu\text{M}$ NaPP1 for 1–48 h. At different intervals during this 48-h incubation, cells were trypsinized and prepared for flow cytometric analysis of cell cycle distribution (top panel) or lysed for analysis of indicated proteins by Western blotting (bottom panel). At 48 h, *v-erbB-as1* cells were washed, resuspended in media without NaPP1, and analyzed similarly.

pocket of *v-erbB*. The resulting ATP-binding pocket has no mammalian homologue, thus assuring high specificity (9). The key feature of this inhibitor is its selectivity for the mutant *v-erbB-as1* kinase (10). In gene-array experiments, NaPP1 had no impact against 126 kinases (11). In addition, selectivity for the analogue sensitive (as compared with the unmanipulated) kinase has now been established for *v-Src*, *c-Fyn*, *CDKII*, *CAMKIIa*, *v-erbB*, *Cl4p*, *Jnk*, *Pho85*, Protein kinase

A, *Apg1*, and *Erk2* (10–20). Most importantly, all wild-type protein kinases in the human and mouse genomes examined to date contain residues larger than Ala or Gly at the conserved “gatekeeper position” (21) and, thus, should not be inhibited by NaPP1. The naphthyl ring of NaPP1 only will fit into kinases with the Ala or Gly residue at the gatekeeper position, providing a molecular basis for the exquisite specificity of NaPP1 for analogue-sensitive kinases. Numerous re-

Fig. 2. NaPP1-mediated apoptosis in arrested 3T3:*v-erbB-as1* cells. 3T3:*v-erbB-as1* cells were seeded in 35-mm dishes at 0.5×10^5 cells/dishes. Cells were incubated with $2 \mu\text{M}$ NaPP1 for up 2 weeks. Media were changed and fresh NaPP1 added every 3 days. At times indicated, cells were trypsinized and analyzed by flow cytometry, terminal deoxynucleotidyl transferase-mediated nick end labeling (TUNEL) staining, or lysed with subsequent Western blotting. **A**, numbers represent the percentage of nonapoptotic cells in G_0/G_1 , S, and G_2/M phases of the cell cycle in NaPP1-treated 3T3:*v-erbB-as1* cells analyzed by flow cytometry. Cells in sub- G_1 fraction were excluded from analysis. **B**, numbers represent the percentage of apoptotic cells. Cells were stained with propidium iodide and cell-cycle data analyzed to quantitate the percentage of cells in sub- G_1 fraction. Error bars indicate the variation between triplicate measurements. **C**, 3T3:*v-erbB-as1* cells were exposed to $2 \mu\text{M}$ NaPP1 for 24 h, after which proteins were separated by SDS-PAGE, transferred to nitrocellulose, and probed with antibodies directed against caspase-3 (which recognizes both pro-caspase 3 and cleaved caspase 3), cleaved caspase 3, Bcl-xL, phospho-Bad (Ser-136), and total Bad. Each lane was loaded with $15 \mu\text{g}$ of protein. **D**, 3T3:*v-erbB-as1* cells were untreated, or treated with $2 \mu\text{M}$ NaPP1 for 7 days. Cytospin preparations were stained with fluorescein-labeled dUTP (green fluorescence) in conjunction with terminal transferase (TUNEL assay) and visualized by confocal laser scanning microscopy. Scale bar corresponds to $100 \mu\text{m}$.



views about this system and its specificity have been published (22–28).

We have previously shown that specific inhibition of *v-erbB-as1* in transformed rodent fibroblasts led to normalization of both morphology and of basal cellular signaling through mitogen-activated protein (MAP) kinase (MAPK) and phosphatidylinositol 3' (PI3) kinase pathways. Despite apparently reversing many features of transformation, treated cells showed proliferation arrest and failed to reenter the cell cycle (10). These data demonstrated that transformed cells became dependent on oncogenic signaling and were subsequently incapable of recovering normal proliferative functions.

In this report, we further characterize the mechanism of proliferation arrest in rodent fibroblast cells transduced with *v-erbB-as1* (3T3:*v-erbB-as1* cells), demonstrating that such arrest is in large part attributable to blockade of signaling through PI3 kinase. Because signaling through PI3 kinase recovered partially after inhibition of *v-erbB-as1*, we asked whether further inhibition of PI3 kinase could enhance the impact of inhibiting *v-erbB-as1*. We demonstrate that inhibitors of *v-erbB-as1* and PI3 kinase show combinatorial efficacy *in vitro* and *in vivo* and that such combinatorial efficacy could be achieved at dosages for each inhibitor that were significantly lower than those required as monotherapy.

Having demonstrated combinatorial efficacy using an idealized kinase inhibitor to treat 3T3:*v-erbB-as1* cells, we then sought to test whether similar combinatorial efficacy could be achieved in human cancer cells using clinically available, albeit less specific inhibitors of

EGFR. We, therefore, tested a mouse xenograft model of glioma using a human glioma cell line dependent on EGFR. Treatment of established flank xenografts using the EGFR inhibitor ZD1839 (Iressa) in combination with an inhibitor of PI3 kinase efficacy again showed combinatorial. These results suggest that agents that show dose-limiting toxicity as monotherapy may potentially be used at lower dosages in combination therapy and support the idea that the combined inhibition of EGFR and PI3 kinase signaling may be effective in glioma, as well as in other human malignancies dependent on signaling through EGFR.

MATERIALS AND METHODS

Cell Culture, Kinase Inhibitors, and Proliferation Assays. All cells were cultured in phenol red-free DMEM supplemented with 10% fetal bovine serum, penicillin, and streptomycin. NIH3T3 cells transduced with *v-erbB* and *v-erbB-as1* were selected as pools using $2.2 \mu\text{g/ml}$ puromycin (10). A human full-length EGFR cDNA in pcDNA3.1 plasmid was kindly provided by Dr. David James (Mayo Clinic, Rochester, MN) digested with *XhoI* and *SaI* and ligated into pWZLhygro vector. NIH3T3 cells transduced with *EGFR* were selected as pools using $500 \mu\text{g/ml}$ hygromycin for 10 days. U87: Δ EGFR cells were kindly provided by Dr. Russ Pieper (University of California at San Francisco Cancer Center, San Francisco, CA). The PP1 analogue 1-Naphthyl PP1 was synthesized as described (29). ZD1839 was synthesized as detailed in Supplementary Fig. 3. LY294002, Platelet-derived growth factor, insulin-like growth factor-I (IGF-I) and 3-(4,5-dimethylthiazol-2-yl)-2,5-diphenyl-tetrazolium bromide were purchased from Sigma Chemical Company (St. Louis,

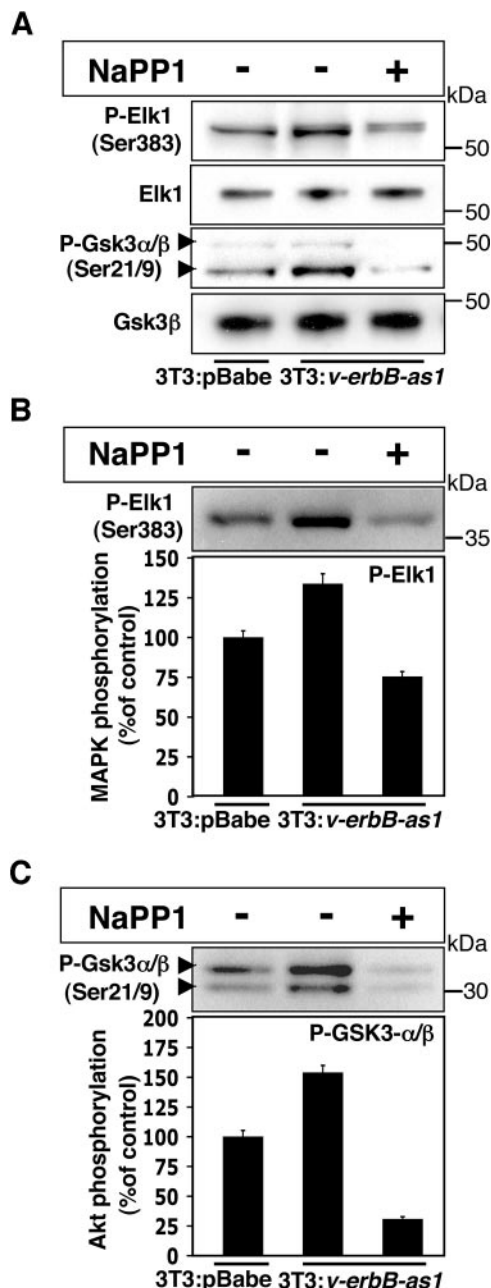


Fig. 3. NaPP1-treatment of 3T3:*v-erbB-as1* cells leads to decreased levels of P-Elk1 and P-Gsk3 α/β and reduced activities of MAP and PI3 kinases. A, NIH3T3 cells transduced with empty vector or with *v-erbB-as1* were treated 2 μ M NaPP1 (36 h). Cells were harvested, lysed, and subjected to immunoblot analysis using the indicated antibodies. B and C, MAPK and Akt kinase activities were assayed by measuring in triplicate the phosphorylation status of Gsk-3 α/β and Elk-1. Cells treated as in A were lysed, and 300 μ g of protein immunoprecipitated with immobilized antibodies that bind to either MAPK or Akt. The immobilized precipitated kinases were then used in kinase assays using Elk-1 (for MAPK) and Gsk-3 α/β (for Akt) as substrates followed by immunoblot analysis using phospho-specific antibodies. Kinase assay products were quantitated using a UMAX PowerLook Scanner and Lab gel software. Bands were normalized using the activity of untreated vector transduced cells as controls.

MO). EGF was purchased from (Roche Molecular Biochemicals, Gaithersburg, MD). Proliferation was quantified by reduction of 3-(4,5-dimethylthiazol-2-yl)-2,5-diphenyl-tetrazolium bromide every day for 1 week after plating. Anti-BrdUrd and propidium iodide flow cytometric analyses were as described previously (10).

Immunoblot Analyses. Details of Western analyses are as previously described (10). Membranes were blotted with one of the following antibodies: 4G10 (Upstate Biotechnology, Waltham, MA), p27 (BD Biosciences Clontech, Palo Alto, CA), P-Erk (Thr202/Tyr204, Erk2, cyclin D1, cyclin A, actin,

P-Elk-1 (Ser-383), Elk-1, and P-EGFR (Ty41173; Santa Cruz Biotechnology, Inc., Santa Cruz, CA), *v-erbB* (30), P-Akt (Ser473), Akt, P-Gsk-3 α/β (Ser21/9), Gsk-3 β , caspase-3, cleaved caspase-3, Bcl-xL, P-Bad (Ser136), Bad, IGF-IR, and P-IGF-IR (Tyr-1146; Cell Signaling, Beverly, MA). EGFR/ Δ EGFR (Ab5; NeoMarkers, Fremont, CA). Bound antibodies were detected with horseradish peroxidase linked antimouse or antirabbit IgG (Amersham Pharmacia Biotech, Arlington Heights, IL), followed by enhanced chemiluminescence (Amersham Pharmacia Biotech, Arlington Heights, IL), and exposure to X-ray film.

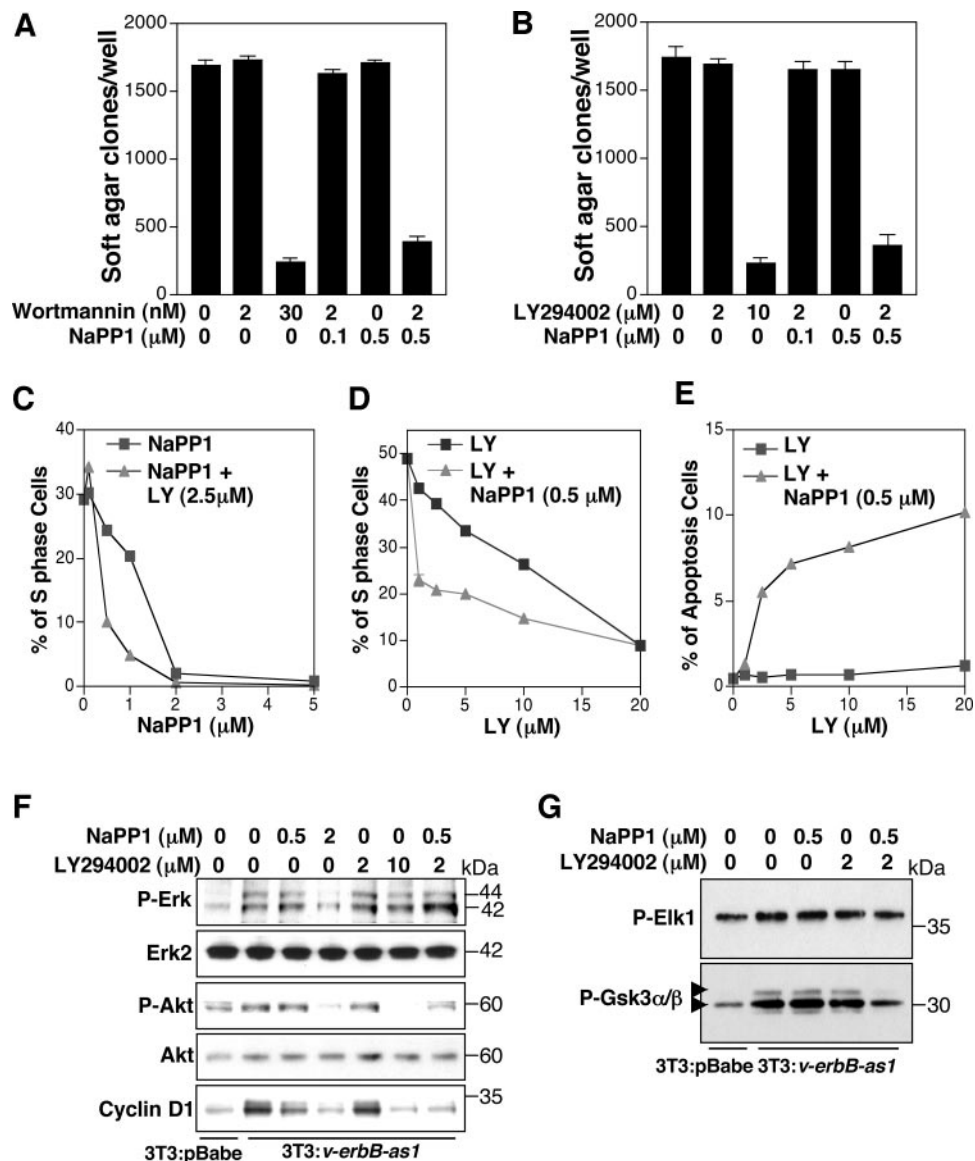
In Vitro Kinase Assays. Akt and MAPK activity assessed by determining the phosphorylation state of their respective substrates, Gsk-3 α/β and Elk-1, using nonradioactive assays (Cell Signaling, Beverly, MA). Briefly, attached cells were treated with NaPP1 2 μ M or vehicle for 36 h and lysed. Equal amounts of protein were immunoprecipitated with immobilized antibodies that bind to either MAPK or Akt. The immobilized precipitated kinases were then used in kinase assays using Elk-1 (for MAPK) and Gsk-3 α/β (for Akt) as substrates, followed by immunoblot analysis using phospho-specific antibodies.

Induction and Assessment of Apoptosis. Cells were seeded in 6-well plates at a density of $5 \times 10^5/\text{cm}^2$ and incubated in the presence or absence of 2 μ M NaPP1. Terminal deoxynucleotidyl transferase-mediated nick end labeling (TUNEL) staining was performed with DeadEnd Fluorometric TUNEL System kit (Promega Corporation, Madison, WI). Cytospins were fixed in 4% paraformaldehyde at room temperature for 20 min, washed three times with PBS, and incubated in permeabilization solution (0.1% Triton-X-100 in PBS) for 5 min. Cells were treated with 100 μ l of equilibration buffer for 10 min and then with TUNEL reaction mixture (to label DNA strand breaks with fluorescein-12-dUTP) for 60 min at 37°C. Nuclei were labeled with To-Pro-3 iodide (Molecular Probes, Eugene, OR) for 30 min at room temperature. Cells were mounted with Vectashield mounting media (Vector Laboratories, Inc., Burlingame, CA) as an antifade and observed using a fluorescent microscope (TET300; Nikon, Tokyo Japan) equipped with a confocal laser scanning system (MR-1024; Bio-Rad, Tokyo, Japan). We performed flow cytometric analysis of propidium iodide-labeled cells to quantitate the percentage of cells in sub G₁ fraction using commercially available software (ModFit; Verity Software, Topsham, ME).

In Vitro and in Vivo Growth Assays. Soft agar experiments were as previously described (10). The care of animals for these studies was in accordance with institutional guidelines. For *in vivo* treatment assays, 1×10^6 3T3:*v-erbB-as1* or U87: Δ EGFR cells were injected s.c. just caudal to the right forelimb in 6–12 week-old female BALB/c *nu/nu* mice (Harlan Sprague Dawley Inc., Madison, WI). After tumors were established (7–8 days), five to six mice per group were randomly allocated to treatment with 10 mg/kg NaPP1 in 50% DMSO (Sigma Chemical Company, St. Louis, MO), 50% DMSO alone (control), LY294002 25 mg/kg, and LY294002 25 mg/kg plus NaPP1 10 mg/kg in a 200- μ l volume, delivered by daily i.p. injection. ZD1839 was administered at 12.5 mg/kg orally once a day. Tumor diameters were measured with calipers at 3 d intervals, and tumor volumes in millimeters cubed were calculated by the following formula: volume = width² \times length/2. Each value represented the mean tumor volume \pm SE obtained from five to six mice.

Histological and Immunohistochemical Analyses. Mice were anesthetized with Nembutal and then perfused with 10 ml of saline followed by 50 ml of 4% paraformaldehyde in PBS. Tumor tissues were removed and fixed in 4% paraformaldehyde in PBS at 4°C for 4 h, followed by overnight incubation in 20% sucrose (in PBS) at 4°C. Specimens were embedded in OCT compound. Sections of 10- μ m thickness were cut and placed on silane-coated slide glasses, and subjected to H&E, BrdUrd, or TUNEL stain. For indirect immunofluorescence, mice were injected with a single dose of BrdUrd (100 mg/kg), and tumors were harvested 2 h later. Sections were incubated in 60% formamide in 2 \times SSC at 54°C for 30 min. DNA was denatured by 2 N HCl in 0.1% Triton X-100 v/v at room temperature for 30 min. Denaturation was neutralized by 0.1 M Na₂B₄O₇·10H₂O (pH 8.5). After washing with PBS, sections were immersed in PBS containing 0.1% Triton X-100 and 5% normal goat serum for 30 min to avoid nonspecific binding of secondary antibodies. Sections were incubated with the rat monoclonal anti-BrdUrd (1:200, Accurate Chemicals) at 4°C overnight followed by the incubation with Cy2-conjugated Donkey antirat IgG (H + L; 1:200 Jackson ImmunoResearch Labs, West Grove, PA) at room temperature for 1 h. For EGFR/ Δ EGFR staining, sections were permeabilized, and incubated with anti-EGFR/ Δ EGFR (Ab5, NeoMarkers, Fremont, CA), washed, and incubated for 1 h in Alexa Four 488 secondary

Fig. 4. NaPP1 and LY294002 show combinatorial efficacy in blocking proliferation, blocking transformation, inducing apoptosis, and inhibiting Akt kinase. *A* and *B*, 3T3:*v-erbB-as1* cells were grown in soft agar using various concentration of Wortmannin, NaPP1, LY294002, or in combination as indicated. Colonies were stained with 100 $\mu\text{g/ml}$ 3-(4,5-dimethylthiazol-2-yl)-2,5-diphenyl-tetrazolium bromide and counted with the aid of a light microscope. Results represent 3 independent plates per experiments point. *C*, 3T3:*v-erbB-as1* cells were treated for 48 h with 0, 0.1, 0.5, 1, 2, and 5 μM NaPP1 alone or in combination with LY294002 (2.5 μM). BrdUrd was added at 42 h. Cells were trypsinized and prepared for flow cytometric analysis of cell-cycle distribution. Percentages of cells in S-phase are shown. *D*, 3T3:*v-erbB-as1* cells were treated with 1, 2.5, 5, 10, and 20 μM LY294002 or in combination with 0.5 μM NaPP1 for 48 h and evaluated as in *C*. *E*, 3T3:*v-erbB-as1* cells were treated for 48 h with 0, 0.1, 2.5, 5, 10, and 20 μM LY294002 alone or in combination with 0.5 μM NaPP1. Numbers represent the percentage of apoptosis cells. Cells were stained with propidium iodide and percentage of cells in sub-G₁ fraction measured. *F* and *G*, 3T3:*v-erbB-as1* cells transduced with empty vector or with *v-erbB-as1* were treated with NaPP1, LY294002, or both at dosages shown (36 h). Cells were harvested, lysed, and subjected to immunoblot analysis using the indicated antibodies (*F*). MAPK and Akt kinase activities were assayed by measuring the phosphorylation status of Gsk-3 α/β and Elk-1 (*G*) as in Fig. 3.



antibodies (Molecular Probes, Eugene, OR). Nuclei were labeled with To-Pro-3 iodide (Molecular Probes, Eugene, OR) for 30 min at room temperature. Sections were mounted with Vectashield mounting media (Vector Laboratories, Inc., Burlingame, CA) as an antifade and observed using a fluorescent microscope (TET300; Nikon, Tokyo, Japan) equipped with a confocal laser scanning system (MR-1024; Bio-Rad, Tokyo, Japan). Additional sections were used to stain for apoptotic cells using the DNA *in situ* nick end-labeling (TUNEL) immunohistochemical method as described above.

RESULTS

NaPP1 Induces Reversible Proliferation Arrest in 3T3:*v-erbB-as1* Cells. We have previously described a mouse model for glioma driven by an S100 β -*v-erbB* transgene (31). Tumors developed in these mice at high penetrance, prompting us to explore chemical genetic modifications of *v-erbB* that should still be capable of driving tumors in transgenic mice, but would allow us to regulate the activity of *v-erbB-as1* using a defined and specific small molecule inhibitor (NaPP1). We, therefore, generated an analogue sensitive allele of *v-erbB* (*v-erbB-as1*) and showed that *v-erbB-as1* was comparable with *v-erbB* in its ability to transform rodent fibroblast cells (10). NaPP1 treatment of 3T3:*v-erbB-as1* cells led to reversal of trans-

formed phenotypes associated with cellular morphology and signaling through both MAP and PI3 kinase pathways (10). Surprisingly, NaPP1 treated 3T3:*v-erbB-as1* cells showed proliferation arrest associated with low levels of cyclin D1 (10). In this report, we explore the mechanistic basis and therapeutic implications of this proliferation arrest. These studies are part of an ongoing effort to characterize *v-erbB-as1* in anticipation of using this allele to generate a genetically engineered mouse model for glioma.

Measurement of proliferation in NIH3T3 cells transformed with *v-erbB* or with *v-erbB-as1* is shown in Fig. 1A. The growth kinetics of these two cell lines were essentially identical in the absence of NaPP1 treatment. Proliferation of 3T3:*v-erbB-as1* cells arrested in response to NaPP1 treatment, whereas proliferation of 3T3:*v-erbB* cells was unaffected (Fig. 1A and Supplementary Fig. 1, A and B). In response to NaPP1 treatment, 3T3:*v-erbB-as1* cells showed growth arrest using dosages of NaPP1 as low as 2 μM (Fig. 1C). Proliferation arrest of NaPP1 treated 3T3:*v-erbB-as1* cells was dependent on NaPP1 because proliferation recovered after washing out the inhibitor (Fig. 1D). The IC₁₀₀ for inhibition of auto-phosphorylation by NaPP1 is \sim 1 μM in 3T3:*v-erbB-as1* cells (10). In contrast, the IC₁₀₀ for inhibition of autophosphorylation of EGFR using the clinically available EGFR

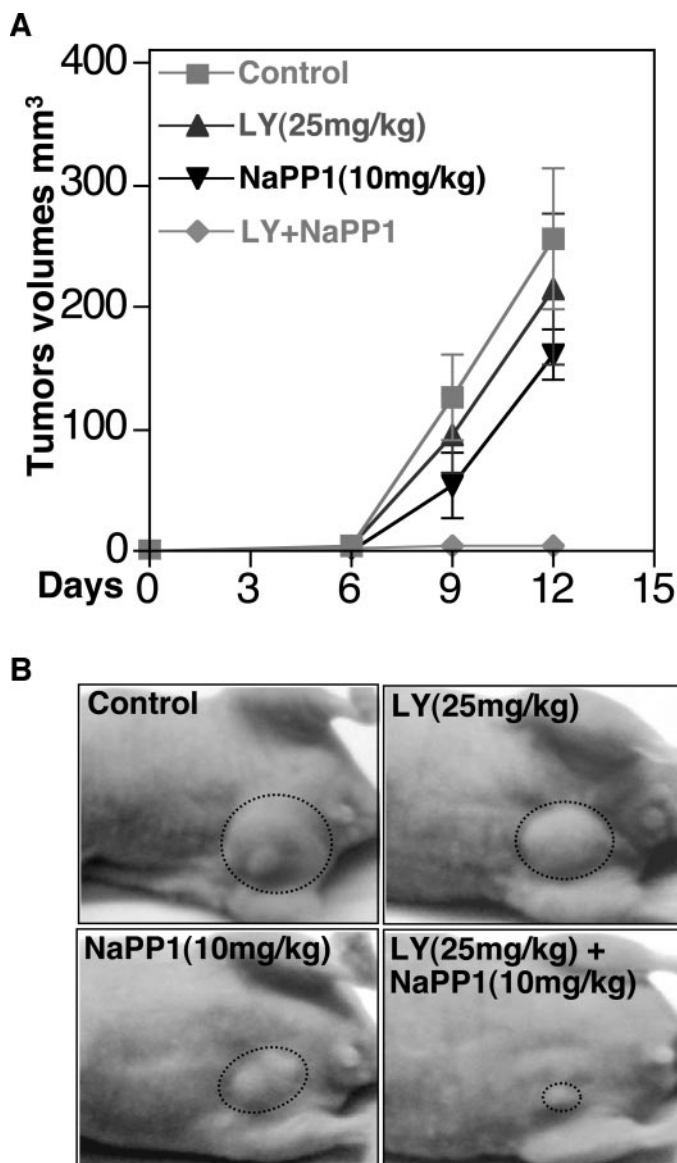


Fig. 5. NaPP1 and LY294002 show combinatorial efficacy on growth of 3T3:*v-erbB-as1* tumor allografts. **A**, 3T3:*v-erbB-as1* cells transduced with *v-erbB-as1* (1×10^6) were injected s.c. in BALB/c *nu/nu* mice and allowed to establish (from 6–10 mm³ in size) for 7 days. The animals were then treated once daily (starting on day 0 of the graph shown) with i.p. injection of DMSO (*control*), 25 mg/kg LY, 10 mg/kg NaPP1, or 25 mg/kg LY plus 10 mg/kg NaPP1. Each data point represents the mean tumor volume \pm SE obtained from six mice. **B**, representative animals after treatment indicated. Circles indicate tumor.

inhibitor ZD1839 ranges from 0.16–0.8 μ M in different cell lines surveyed (reviewed in Ref. 32).

To assess the role of IGF-I and EGF signal pathways in 3T3:*v-erbB-as1* cells, we treated these cells with IGF-I or with EGF and measured phosphorylation status of Akt and of Erk over time. NIH3T3 cells have little to no expression of EGFR (Supplementary Fig. 2A). Consistent with this low level of expression, EGF stimulation of these cells had little impact on levels of phospho-Erk or phospho-Akt (Supplementary Fig. 2A). In contrast, IGF stimulation of 3T3:*v-erbB-as1* cells, demonstrated a modest increase in Phospho-Akt.

Apoptosis in Arrested NaPP1-Treated 3T3:*v-erbB-as1* Cells. We maintained 3T3:*v-erbB-as1* cells in NaPP1 (changing the media every three days) for up to 2 weeks without observing recovery of proliferative capacity (Fig. 2A). We used morphology, TUNEL, and flow cytometry to measure apoptosis in arrested *v-erbB-as1* cells. By

each of these assays, NaPP1 treatment of 3T3:*v-erbB-as1* cells led to increased apoptosis (Fig. 2, B–D). Apoptosis in these cells was associated with activation of caspase-3, decreased phosphorylation of BAD at serine 136, down-regulation of Bcl-xL, and the characteristic morphological features of apoptosis (33).

Decreased Signaling through PI3 Kinase Contributes to Proliferation Arrest in NaPP1-Treated 3T3:*v-erbB-as1* Cells. We have shown previously that NaPP1 treatment of 3T3:*v-erbB-as1* cells initially caused a reduction in the levels of activated MAP and Akt kinases, returning by 36 h to levels comparable with those observed in proliferating vector-transduced 3T3 cells (10). Despite the apparent normalization of signaling through these two pathways, NaPP1 treated 3T3:*v-erbB-as1* cells failed to proliferate, showed reduced levels of A and D type cyclins, and increased levels of p27 (10). To further characterize the impact of NaPP1 on signaling through *v-erbB-as1*, we examined the phosphorylation status of the MAPK substrate Elk 1 and of the Akt kinase substrates Gsk-3 α/β . As shown in Fig. 3A, phosphorylation of Gsk-3 α/β was impacted more than phosphorylation of Elk1 in comparing NaPP1 treated 3T3:*v-erbB-as1* cells (Fig. 3A, Lane 3) with untreated, vector-transduced 3T3 cells (Fig. 3A, Lane 1). We next measured the activities of MAPK and Akt kinase using Elk1- and Gsk-3 β -derived substrates. Under these conditions, NaPP1 treatment impacted the activity of Akt kinase more than that of MAPK (Fig. 3, B and C).

NaPP1 and LY294002 Show Combinatorial Efficacy in 3T3:*v-erbB-as1* Cells. Collectively, data from Fig. 3 suggest that Akt kinase activity was reduced in response to NaPP1 and that the proliferation arrest observed in 3T3:*v-erbB-as1* cells resulted, in large part, from reduced signaling through PI3 kinase. We, therefore, asked whether NaPP1, in combination with inhibitors of PI3 kinase, could show a combinatorial effect in these cells. Both Wortmannin and LY294002 showed combinatorial efficacy when used together with NaPP1 *in vitro* (Fig. 4, A and B). The combination of NaPP1 with either Wortmannin or LY294002 blocked the growth of 3T3:*v-erbB-as1* cells in soft agar at dosages substantially lower than that achieved using any of these drug alone. We then measured proliferation of 3T3:*v-erbB-as1* cells in response to a fixed dose of LY294002, while varying the dose of NaPP1 (Fig. 4C). Shown in Fig. 4D is the reciprocal experiment using a fixed dose of NaPP1 and varying the dose of LY294002. Combination therapy using both LY294002 and NaPP1 led to increased levels of apoptosis in comparison with monotherapy (Fig. 4E). Importantly, using doses of NaPP1 (0.5 μ M) and LY294002 (2 μ M), which as monotherapy only modestly affected the level of phospho-Akt, we showed that combination therapy with NaPP1 and LY294002 impacted both the level and activity of phospho-Akt, with minimal effects on phospho-Erk (Fig. 4, F and G).

To determine whether these *in vitro* observations could be validated *in vivo*, we assessed the impact of combinatorial therapy using LY294002 and NaPP1 to treat established 3T3:*v-erbB-as1* cell allografts in immunocompromised mice. A dramatic combinatorial effect of these agents in halting growth of allografted tumor is shown in Fig. 5A. The response of representative individual tumors to single and combination therapy is shown in Fig. 5B.

Combinatorial Efficacy through Inhibition of EGFR and PI3 Kinases in a Human Brain Tumor Cell Line. LY294002 has limited potential for clinical development, in part, because of toxicity (34). Importantly, observations in Figs. 4 and 5 suggest that this compound or similar molecules could potentially be used at subtoxic dosages if administered in combination with inhibitors of receptor tyrosine kinases. To assess the generalizability of these observations to human tumors, we asked whether similar combinatorial efficacy could be achieved in human brain tumor cell lines, using combination therapy with inhibitors of PI3 and EGFR kinases. Astrocytomas

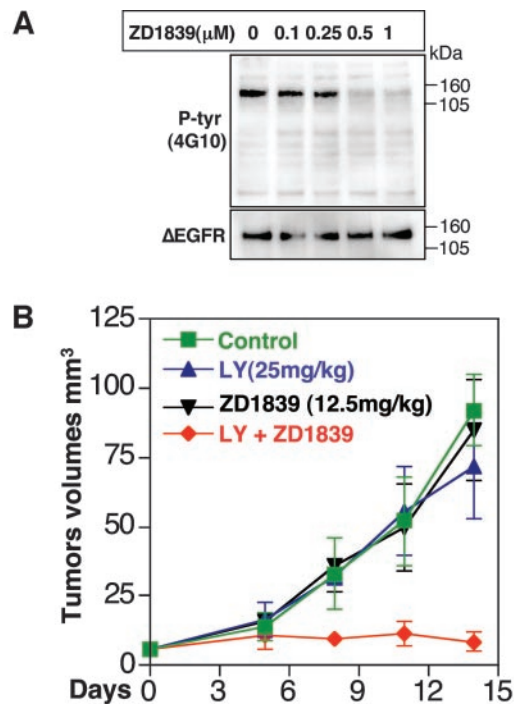
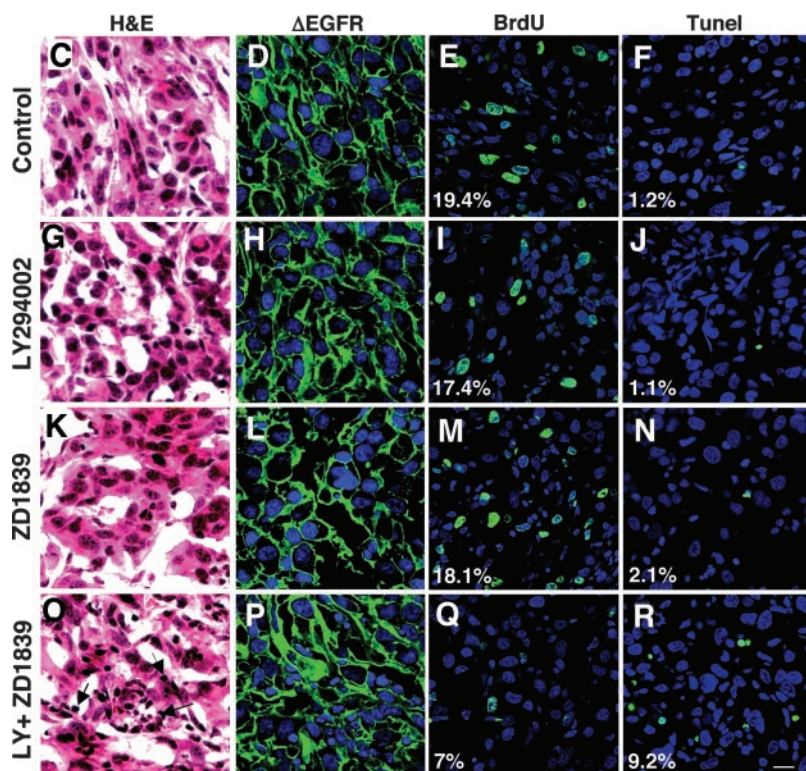


Fig. 6. ZD1839 and LY294002 show combinatorial efficacy on growth of U87: Δ EGFR tumor xenografts. **A**, U87: Δ EGFR cells were treated with 0.1–1 μ M ZD1839 for 24 h. Cells were harvested and lysed. Cellular proteins were resolved by 4–20% SDS-PAGE, transferred to nitrocellulose, and immunoblotted with antibodies to P-Tyr (4G10) and to EGFR/EGFRv3 (Ab5). **B**, U87MG cells transduced with Δ EGFR (1×10^6) were injected s.c. in BALB/c *nu/nu* mice and allowed to establish for 8 days (6–10 mm³ in size). Starting on *day 0* of the graph shown, animals with established tumors were treated once daily with either DMSO (control-delivered i.p.), 25 mg/kg LY delivered i.p., 12.5 mg/kg ZD1839 administered p.o., or 25 mg/kg LY plus 12.5 mg/kg ZD1839. Each *data point* represents the mean tumor volume \pm SE obtained from five mice. **C–R**, ZD1839 and LY294002 inhibit proliferation and induce apoptosis. On day 14 of treatment, two mice in each group were randomly selected and pulsed with BrdUrd (*BrdU*) before tumor harvesting. Tumor sections were stained with H&E (**C**, **G**, **K**, and **O**). *Arrows* in **O** show increased pyknotic nuclei in response to LY + ZD1839. Tumor sections were also stained with an antibody to EGFR/ Δ EGFR (Ab5; *green* in **D**, **H**, **L**, and **P**), antibody to BrdUrd (*green* in **E**, **I**, **M**, and **Q**), or with fluorescein-labeled (*green*) dUTP in conjunction with a terminal deoxynucleotidyl transferase-mediated nick end labeling (TUNEL) assay (*green* in **F**, **J**, **N**, and **R**). Nuclei were counter-stained with To-Pro-3 iodide (*blue*) and visualized by confocal laser scanning microscopy. BrdUrd-positive and TUNEL-positive nuclei were counted in 10 high-power microscopic fields. *Numbers* denote the percentage of BrdUrd-positive and TUNEL-positive nuclei relative to the total number of tumor cell nuclei in the same fields. *Scale bar* corresponds to 100 μ m.



frequently amplify *EGFR*, a genetic lesion not observed in astrocytoma derived cell lines (35–37). U87MG is a human glioma cell line in which an activated tumor-derived allele of *EGFR* (Δ EGFR; also called *EGFRvIII*) leads to increased malignancy (38). Importantly, treatment of U87: Δ EGFR xenografts with antibody to Δ EGFR blocked growth *in vivo* (39, 40), and treatment of these cells with LY294002 led to proliferation arrest *in vitro* (41). We, therefore, treated U87: Δ EGFR cells with ZD1839, an inhibitor of EGFR with demonstrated efficacy against Δ EGFR. Shown in Fig. 6A is the

observation that ZD1839 blocked tyrosine phosphorylation of Δ EGFR in U87: Δ EGFR cells. We next established U87: Δ EGFR allografts in immunocompromised mice, and treated the mice with ZD1839, LY294002, or a combination of ZD1839 and LY294002. Again, Fig. 6B shows a dramatic combinatorial effect of ZD1839 and LY294002 in halting growth of the allografted tumor. Combinatorial therapy led to increased apoptosis as indicated by pyknotic nuclei (Fig. 6, **C**, **G**, **K**, and **O**) and increased TUNEL staining (Fig. 6, compare **R** with **F**, **J**, and **N**). Combinatorial therapy also led to decreased proliferation

(Fig. 6, compare Q with E , I , and M). Levels of EGFR were not different among treated and untreated tumors (Fig. 6, D , H , L and P). These results extend and validate similar data presented in Fig. 5, showing combinatorial efficacy of NaPP1 and LY294002 in treatment of *v-erbB-as1* tumor allografts.

DISCUSSION

Combination Therapy Directed at Two Nodes in a Signaling Pathway: Implications for Human Cancer. Cancer therapy traditionally combines cytotoxic agents, or a cytotoxic agent with a biologically active agent. Our experiments demonstrate that biologically based therapies, which target two points within a complex signaling cascade, may effectively cooperate in the preclinical treatment of cancer. This cooperative effect was seen at dosages for each compound that were significantly lower than that required for use as monotherapy. These observations suggest that combinatorial therapy using biologically targeted agents may allow the use of relatively toxic agents at concentrations below those reported to elicit dose-limiting side effects, and argue that inhibitors of EGFR, in combination with inhibitors of PI3 kinase may show efficacy in patients with glioma, and with other tumors in which both EGFR and PI3 kinase signaling are active.

The observation that both NaPP1 and ZD1839 cooperate with LY294002 raises important clinical and scientific questions. Although the interaction of NaPP1 with *v-erbB-as1* is quite specific, the interaction of LY294002 with PI3 kinase is much less specific. PI3 kinases are a family of lipid kinases that phosphorylate phosphatidylinositol at the D_3 position. The impact of PI3 kinase activation is mediated through a complex signaling pathway (34). LY294002 inhibits a number of PI3 kinase isoforms and also inhibits molecules with homology to PI3 kinase, including the mTOR kinase, which signals, in part, downstream from PI3 kinase and shares homology with the PI3 kinases. PI3 kinase generates phosphatidylinositol 3,4,5-trisphosphate, resulting in 3-phosphoinositide-dependent protein kinase-1-mediated activation of AKT, a serine-threonine protein kinase. AKT is known to phosphorylate at least 13 substrates, including the proapoptotic factors BAD and Casp9 (42–44), the growth-inhibitory protein glycogen synthase kinase 3 β (Gsk-3 β), the forkhead transcription factor FKHLR1 (45–47), and the TSC2 protein, which negatively regulates the translation regulatory protein mTOR (reviewed in Ref. 48). Clearly, future experiments that test inhibition of *v-erbB-as1* or EGFR in combination with selective inhibitors for specific isoforms of PI3 kinases, and in combination with inhibitors of individual proteins that signal downstream of PI3 kinase, will be important to clarify the contributions of each to the cooperativity observed in combining inhibitors of EGFR with inhibitors of PI3 kinase. In addition, animal models of glioma, based both on *v-erbB*, *v-erbB-as1*, and on *EGFR/ΔEGFR*, will serve as important tools for evaluating the efficacy of combination therapy against preclinical models of glioma.

ACKNOWLEDGMENTS

We thank David James and Russ Pieper for reagents and David Threadgill for useful comments. We acknowledge David Stokoe and Doug Hanahan for critical review of the manuscript. W. A. W. is a Kimmel Scholar.

REFERENCES

- Druker, B. J. Perspectives on the development of a molecularly targeted agent. *Cancer Cell*, *1*: 31–36, 2002.
- Davies, S. P., Reddy, H., Caivano, M., and Cohen, P. Specificity and mechanism of action of some commonly used protein kinase inhibitors. *Biochem. J.*, *351*: 95–105, 2000.

- Drevs, J., Medinger, M., Schmidt-Gersbach, C., Weber, R., and Unger, C. Receptor tyrosine kinases: the main targets for new anticancer therapy. *Curr. Drug Targets*, *4*: 113–121, 2003.
- Manning, G., Whyte, D. B., Martinez, R., Hunter, T., and Sudarsanam, S. The protein kinase complement of the human genome. *Science (Wash. DC)*, *298*: 1912–1934, 2002.
- Torrance, C. J., Jackson, P. E., Montgomery, E., Kinzler, K. W., Vogelstein, B., Wissner, A., Nunes, M., Frost, P., and Discifani, C. M. Combinatorial chemoprevention of intestinal neoplasia. *Nat. Med.*, *6*: 1024–1028, 2000.
- Ritland, S. R., Gendler, S. J., Burgart, L. J., Fry, D. W., Nelson, J. M., Bridges, A. J., Andress, L., and Karnes, W. E., Jr. Inhibition of epidermal growth factor receptor tyrosine kinase fails to suppress adenoma formation in ApcMin mice but induces duodenal injury. *Cancer Res.*, *60*: 4678–4681, 2000.
- Roberts, R. B., Min, L., Washington, M. K., Olsen, S. J., Settle, S. H., Coffey, R. J., and Threadgill, D. W. Importance of epidermal growth factor receptor signaling in establishment of adenomas and maintenance of carcinomas during intestinal tumorigenesis. *Proc. Natl. Acad. Sci. USA*, *99*: 1521–1526, 2002.
- Downward, J., Yarden, Y., Mayes, E., Scrace, G., Totty, N., Stockwell, P., Ullrich, A., Schlessinger, J., and Waterfield, M. D. Close similarity of epidermal growth factor receptor and *v-erb-B* oncogene protein sequences. *Nature (Lond.)*, *307*: 521–527, 1984.
- Liu, Y., Bishop, A., Witucki, L., Kraybill, B., Shimizu, E., Tsien, J., Ubersax, J., Blethrow, J., Morgan, D. O., and Shokat, K. M. Structural basis for selective inhibition of Src family kinases by PP1. *Chem. Biol.*, *6*: 671–678, 1999.
- Fan, Q. W., Zhang, C., Shokat, K. M., and Weiss, W. A. Chemical genetic blockade of transformation reveals dependence on aberrant oncogenic signaling. *Curr. Biol.*, *12*: 1386–1394, 2002.
- Bishop, A. C., Ubersax, J. A., Petsch, D. T., Matheos, D. P., Gray, N. S., Blethrow, J., Shimizu, E., Tsien, J. Z., Schultz, P. G., Rose, M. D., Wood, J. L., Morgan, D. O., and Shokat, K. M. A chemical switch for inhibitor-sensitive alleles of any protein kinase. *Nature (Lond.)*, *407*: 395–401, 2000.
- Gillespie, P. G., Gillespie, S. K., Mercer, J. A., Shah, K., and Shokat, K. M. Engineering of the myosin- $\text{i}\beta$ nucleotide-binding pocket to create selective sensitivity to N(6)-modified ADP analogs. *J. Biol. Chem.*, *274*: 31373–31381, 1999.
- Liu, Y., Witucki, L. A., Shah, K., Bishop, A. C., and Shokat, K. M. Src-Abl tyrosine kinase chimeras: replacement of the adenine binding pocket of *c-Abl* with *v-Src* to swap nucleotide and inhibitor specificities. *Biochemistry*, *39*: 14400–14408, 2000.
- Habelhah, H., Shah, K., Huang, L., Burlingame, A. L., Shokat, K. M., and Ronai, Z. Identification of new JNK substrate using ATP pocket mutant JNK and a corresponding ATP analogue. *J. Biol. Chem.*, *276*: 18090–18095, 2001.
- Wang, H., Shimizu, E., Tang, Y. P., Cho, M., Kyin, M., Zuo, W., Robinson, D. A., Alaimo, P. J., Zhang, C., Morimoto, H., Zhuo, M., Feng, R., Shokat, K. M., and Tsien, J. Z. Inducible protein knockout reveals temporal requirement of CaMKII reactivation for memory consolidation in the brain. *Proc. Natl. Acad. Sci. USA*, *100*: 4287–4292, 2003.
- Ehlen, S. T., Kumar, N. V., Shah, K., Henderson, M. J., Watts, C. K., Shokat, K. M., and Weber, M. J. Identification of novel ERK2 substrates through use of an engineered kinase and ATP analogs. *J. Biol. Chem.*, *278*: 14926–14935, 2003.
- Abeliovich, H., Zhang, C., Dunn, W. A., Jr., Shokat, K. M., and Klionsky, D. J. Chemical genetic analysis of *Atg1* reveals a non-kinase role in the induction of autophagy. *Mol. Biol. Cell*, *14*: 477–490, 2003.
- Niswender, C. M., Ishihara, R. W., Judge, L. M., Zhang, C., Shokat, K. M., and McKnight, G. S. Protein engineering of protein kinase A catalytic subunits results in the acquisition of novel inhibitor sensitivity. *J. Biol. Chem.*, *277*: 28916–28922, 2002.
- Holt, J. R., Gillespie, S. K., Provance, D. W., Shah, K., Shokat, K. M., Corey, D. P., Mercer, J. A., and Gillespie, P. G. A chemical-genetic strategy implicates myosin-1c in adaptation by hair cells. *Cell*, *108*: 371–381, 2002.
- Carroll, A. S., Bishop, A. C., DeRisi, J. L., Shokat, K. M., and O'Shea, E. K. Chemical inhibition of the Pho85 cyclin-dependent kinase reveals a role in the environmental stress response. *Proc. Natl. Acad. Sci. USA*, *98*: 12578–12583, 2001.
- Buzko, O., and Shokat, K. M. A kinase sequence database: sequence alignments and family assignment. *Bioinformatics*, *18*: 1274–1275, 2002.
- Specht, K. M., and Shokat, K. M. The emerging power of chemical genetics. *Curr. Opin. Cell Biol.*, *14*: 155–159, 2002.
- Shokat, K. M., and Velleca, M. Novel chemical genetic approaches to the discovery of signal transduction inhibitors. *Drug Discov. Today*, *7*: 872–879, 2002.
- Shogren-Knaak, M. A., Alaimo, P. J., and Shokat, K. M. Recent advances in chemical approaches to the study of biological systems. *Annu. Rev. Cell Dev. Biol.*, *17*: 405–433, 2001.
- Alaimo, P. J., Shogren-Knaak, M. A., and Shokat, K. M. Chemical genetic approaches for the elucidation of signaling pathways. *Curr. Opin. Chem. Biol.*, *5*: 360–367, 2001.
- Bishop, A. C., Buzko, O., and Shokat, K. M. Magic bullets for protein kinases. *Trends Cell Biol.*, *11*: 167–172, 2001.
- Bishop, A., Buzko, O., Heyeck-Dumas, S., Jung, I., Kraybill, B., Liu, Y., Shah, K., Ulrich, S., Witucki, L., Yang, F., Zhang, C., and Shokat, K. M. Unnatural ligands for engineered proteins: new tools for chemical genetics. *Annu. Rev. Biophys. Biomol. Struct.*, *29*: 577–606, 2000.
- Bishop, A. C., Shah, K., Liu, Y., Witucki, L., Kung, C., and Shokat, K. M. Design of allele-specific inhibitors to probe protein kinase signaling. *Curr. Biol.*, *8*: 257–266, 1998.
- Bishop, A. C., and Shokat, K. M. Acquisition of inhibitor-sensitive protein kinases through protein design. *Pharmacol. Ther.*, *82*: 337–346, 1999.
- Schatzman, R. C., Evan, G. I., Privalsky, M. L., and Bishop, J. M. Orientation of the *v-erb-B* gene product in the plasma membrane. *Mol. Cell Biol.*, *6*: 1329–1333, 1986.

31. Weiss, W. A., Burns, M. J., Hackett, C., Aldape, K., Hill, J. R., Kuriyama, H., Kuriyama, N., Milshcheyn, N., Roberts, T., Wendland, M. F., DePinho, R., and Israel, M. A. Genetic determinants of malignancy in a mouse model for oligodendroglioma. *Cancer Res.*, *63*: 1589–1595, 2003.
32. Woodburn, J. R. The epidermal growth factor receptor and its inhibition in cancer therapy. *Pharmacol. Ther.*, *82*: 241–250, 1999.
33. Hacker, G. The morphology of apoptosis. *Cell Tissue Res.*, *301*: 5–17, 2000.
34. Vivanco, I., and Sawyers, C. L. The phosphatidylinositol 3-kinase AKT pathway in human cancer. *Nat. Rev. Cancer*, *2*: 489–501, 2002.
35. Libermann, T. A., Nusbaum, H. R., Razon, N., Kris, R., Lax, I., Soreq, H., Whittle, N., Waterfield, M. D., Ullrich, A., and Schlessinger, J. Amplification, enhanced expression and possible rearrangement of *EGF* receptor gene in primary human brain tumours of glial origin. *Nature (Lond.)*, *313*: 144–147, 1985.
36. Wong, A. J., Ruppert, J. M., Bigner, S. H., Grzeschik, C. H., Humphrey, P. A., Bigner, D. S., and Vogelstein, B. Structural alterations of the epidermal growth factor receptor gene in human gliomas. *Proc. Natl. Acad. Sci. USA*, *89*: 2965–2969, 1992.
37. Ekstrand, A. J., James, C. D., Cavenee, W. K., Seliger, B., Pettersson, R. F., and Collins, V. P. Genes for epidermal growth factor receptor, transforming growth factor α , and epidermal growth factor and their expression in human gliomas *in vivo*. *Cancer Res.*, *51*: 2164–2172, 1991.
38. Nishikawa, R., Ji, X. D., Harmon, R. C., Lazar, C. S., Gill, G. N., Cavenee, W. K., and Huang, H. J. A mutant epidermal growth factor receptor common in human glioma confers enhanced tumorigenicity. *Proc. Natl. Acad. Sci. USA*, *91*: 7727–7731, 1994.
39. Mishima, K., Johns, T. G., Luwor, R. B., Scott, A. M., Stockert, E., Jungbluth, A. A., Ji, X. D., Suvarna, P., Voland, J. R., Old, L. J., Huang, H. J., and Cavenee, W. K. Growth suppression of intracranial xenografted glioblastomas overexpressing mutant epidermal growth factor receptors by systemic administration of monoclonal antibody (mAb) 806, a novel monoclonal antibody directed to the receptor. *Cancer Res.*, *61*: 5349–5354, 2001.
40. Luwor, R. B., Johns, T. G., Murone, C., Huang, H. J., Cavenee, W. K., Ritter, G., Old, L. J., Burgess, A. W., and Scott, A. M. Monoclonal antibody 806 inhibits the growth of tumor xenografts expressing either the de2–7 or amplified epidermal growth factor receptor (*EGFR*) but not wild-type *EGFR*. *Cancer Res.*, *61*: 5355–5361, 2001.
41. Narita, Y., Nagane, M., Mishima, K., Huang, H. J., Furnari, F. B., and Cavenee, W. K. Mutant epidermal growth factor receptor signaling down-regulates p27 through activation of the phosphatidylinositol 3-kinase/Akt pathway in glioblastomas. *Cancer Res.*, *62*: 6764–6769, 2002.
42. del Peso, L., Gonzalez-Garcia, M., Page, C., Herrera, R., and Nunez, G. Interleukin-3-induced phosphorylation of BAD through the protein kinase Akt. *Science (Wash. DC)*, *278*: 687–689, 1997.
43. Datta, S. R., Dudek, H., Tao, X., Masters, S., Fu, H., Gotoh, Y., and Greenberg, M. E. Akt phosphorylation of BAD couples survival signals to the cell-intrinsic death machinery. *Cell*, *91*: 231–241, 1997.
44. Cardone, M. H., Roy, N., Stennicke, H. R., Salvesen, G. S., Franke, T. F., Stanbridge, E., Frisch, S., and Reed, J. C. Regulation of cell death protease caspase-9 by phosphorylation. *Science (Wash. DC)*, *282*: 1318–1321, 1998.
45. Cross, D. A., Alessi, D. R., Cohen, P., Andjelkovich, M., and Hemmings, B. A. Inhibition of glycogen synthase kinase-3 by insulin mediated by protein kinase B. *Nature (Lond.)*, *378*: 785–789, 1995.
46. Biggs, W. H., 3rd, Meisenhelder, J., Hunter, T., Cavenee, W. K., and Arden, K. C. Protein kinase B/Akt-mediated phosphorylation promotes nuclear exclusion of the winged helix transcription factor FKHR1. *Proc. Natl. Acad. Sci. USA*, *96*: 7421–7426, 1999.
47. Brunet, A., Bonni, A., Zigmond, M. J., Lin, M. Z., Juo, P., Hu, L. S., Anderson, M. J., Arden, K. C., Blenis, J., and Greenberg, M. E. Akt promotes cell survival by phosphorylating and inhibiting a Forkhead transcription factor. *Cell*, *96*: 857–868, 1999.
48. Kwiatkowski, D. J. Tuberous Sclerosis: from Tubers to mTOR. *Ann. Hum. Genet.*, *67*: 87–96, 2003.